

2020-04-21

# EIMS Fragmentation and detection of autoxidation products of 2,6,10,14tetramethyl7(3methylpent4enyl)pentadec in Arctic sediments

Rontani, J

<http://hdl.handle.net/10026.1/15595>

---

10.1002/rcm.8816

Rapid Communications in Mass Spectrometry

Wiley

---

*All content in PEARL is protected by copyright law. Author manuscripts are made available in accordance with publisher policies. Please cite only the published version using the details provided on the item record or document. In the absence of an open licence (e.g. Creative Commons), permissions for further reuse of content should be sought from the publisher or author.*



# EIMS Fragmentation and detection of autoxidation products of 2,6,10,14-tetramethyl-7-(3-methylpent-4-enyl)-pentadec-5-ene in Arctic sediments

Journal:	<i>Rapid Communications in Mass Spectrometry</i>
Manuscript ID	RCM-20-0078.R1
Wiley - Manuscript type:	Research Article
Date Submitted by the Author:	17-Apr-2020
Complete List of Authors:	RONTANI, Jean-François; M.I.O., Aix-Marseille University Smik, Lukas; Plymouth University Belt, Simon; Plymouth University
Keywords:	Autoxidation, HBI diene, (Z and E) 2,6,10,14-tetramethyl-7-(3-methylpent-4-enyl)-pentadec-5-en-4-ol TMS derivatives, EIMS fragmentations, Sediments
Abstract:	2,6,10,14-Tetramethyl-7-(3-methylpent-4-enyl)-pentadec-5(Z/E)-en-4-ols were identified after autoxidation of the HBI alkene 2,6,10,14-tetramethyl-7-(3-methylpent-4-enyl)-pentadec-5-ene. CID-MS/MS analyses and accurate mass measurement allowed EIMS fragmentations of their TMS derivatives to be elucidated. Some specific fragment ions and chromatographic retention times were also useful for further characterization. As an application of some of the described fragmentations, TMS derivatives of these metabolites were characterized and quantified in MRM mode in Arctic sediments.

SCHOLARONE™  
Manuscripts

# EIMS Fragmentation and detection of autoxidation products of 2,6,10,14-tetramethyl-7-(3-methylpent-4-enyl)-pentadec-5-ene in Arctic sediments

Jean-François Rontani<sup>1\*</sup>, Lukas Smik<sup>2</sup> and Simon T. Belt<sup>2</sup>

<sup>1</sup> Aix Marseille Univ, Université de Toulon, CNRS, IRD, MIO UM 110, Marseille, France, 13288, Marseille, France.

<sup>2</sup> Biogeochemistry Research Centre, School of Geography, Earth and Environmental Sciences, University of Plymouth, Drake Circus, Plymouth, ~~Devon~~ PL4 8AA, UK.

\* Corresponding author. Tel.: +33-4-86-09-06-02; fax: +33-4-91-82-96-41. E-mail address: jean-francois.rontani@mio.osupytheas.fr (J.-F. Rontani).

## Abstract

### RATIONALE:

Some highly branched isoprenoid (HBI) alkenes are commonly used as proxies for palaeoceanographic reconstructions. However, there is a need to identify compounds that are sufficiently stable and abundant to be used as tracers of HBI oxidation in sediments. 2,6,10,14-tetramethyl-7-(3-methylpent-4-enyl)-pentadec-5(*Z/E*)-en-4-ols resulting from 2,6,10,14-tetramethyl-7-(3-methylpent-4-enyl)-pentadec-5-ene appear to be useful for [a this](#) purpose.

### METHODS:

Comparison of EIMS mass spectra and retention times with [those of](#) standards allowed formal identification of autoxidation products of 2,6,10,14-tetramethyl-7-(3-methylpent-4-enyl)-pentadec-5-ene. EIMS fragmentations of TMS ethers of the main oxidation products (2,6,10,14-tetramethyl-7-(3-methylpent-4-enyl)-pentadec-5(*Z/E*)-en-4-ols) were deduced by GC-~~EI~~-MS, low energy CID-MS/MS and accurate mass measurements. These compounds were then quantified in Arctic sediment samples in [MS/MS](#) MRM mode using transitions based on the main fragmentation pathways elucidated.

### RESULTS:

2,6,10,14-Tetramethyl-7-(3-methylpent-4-enyl)-pentadec-5(*Z/E*)-en-4-ols were identified after autoxidation of the HBI alkene 2,6,10,14-tetramethyl-7-(3-methylpent-4-enyl)-pentadec-5-ene. Low energy CID-MS/MS analyses and accurate mass measurement allowed [the b](#)EIMS fragmentation [pathways](#) of their TMS derivatives to be elucidated. Some specific fragment ions and chromatographic retention times were also useful for further characterization. As an application of some of the described fragmentations, TMS derivatives of these metabolites were characterized and quantified in MRM mode in Arctic sediments.

1  
2  
3  
4  
5  
6  
7  
8  
9  
10  
11  
12  
13  
14  
15  
16  
17  
18  
19  
20  
21  
22  
23  
24  
25  
26  
27  
28  
29  
30  
31  
32  
33  
34  
35  
36  
37  
38  
39  
40  
41  
42  
43  
44  
45  
46  
47  
48  
49  
50  
51  
52  
53  
54  
55  
56  
57  
58  
59  
60

53  
  
54  
  
55  
  
56  
  
57  
  
58  
  
59  
  
60  
  
61  
  
62  
  
63  
  
64

**CONCLUSIONS:**

Due to: (i) their production in high proportion during autoxidation of their parent HBI diene, (ii) their apparent stability in sediments, and (iii) their specific EIMS fragmentations, (*Z* and *E*) 2,6,10,14-tetramethyl-7-(3-methylpent-4-enyl)-pentadec-5-en-4-ol TMS derivatives appeared to be useful tracers of HBI autoxidation in sediments.

**RUNNING TITLE:** Mass fragmentations of autoxidation products of an HBI diene.

**KEYWORDS:** Autoxidation; HBI diene; (*Z* and *E*) 2,6,10,14-tetramethyl-7-(3-methylpent-4-enyl)-pentadec-5-en-4-ol TMS derivatives; EIMS fragmentation; Sediments.

## 1. INTRODUCTION

Highly branched isoprenoid alkenes (HBIs), which are biosynthesized by a relatively small number of diatom taxa belonging to the *Haslea*, *Navicula*, *Pleurosigma*, *Berkeleya*, *Rhizosolenia* and *Pseudosolenia* genera,<sup>1-8</sup> are nonetheless common constituents of marine and lacustrine sediments.<sup>9-11</sup> Due to their source specificity and relative stability within the geological record, some HBIs are now commonly used as proxies for palaeoceanographic reconstructions, especially in the Polar Regions.<sup>12</sup> Some mono- and di-unsaturated HBIs have been proposed as proxy measures of past seasonal sea ice in the Arctic and Antarctic,<sup>5,12</sup> while some tri-unsaturated HBIs have been proposed as possible proxies for the open waters of the marginal ice zone in the Polar Regions.<sup>12</sup>

Application of such proxies requires careful consideration of alteration and preservation between their source and sedimentary environments. According to the number, the position and the ionization potential of their double bonds and the strength of their allylic C–H bonds, HBIs may be affected more or less intensively by photooxidation in the sunlit layer of oceans<sup>13,14</sup> and by autoxidation in oxic environments such as the water column and surficial sediments,<sup>14,15</sup> prior to being longer-term preserved in anoxic sediments.<sup>12</sup> Although some oxidation tracers of individual HBIs have been identified and characterised,<sup>15-17</sup> they are often either too susceptible to secondary oxidation (e.g. for tri-unsaturated HBIs with *bis*-allylic double bonds<sup>15</sup>) or are produced in too low proportion (e.g. for mono- and di-unsaturated HBIs<sup>16,17</sup>) to permit meaningful quantification. There is thus a real need to identify HBI oxidation products that are sufficiently stable and abundant to estimate the impact of oxidative degradation processes on the preservation of these lipid biomarkers in marine environments.

The present work focuses on the oxidation of 2,6,10,14-tetramethyl-7-(3-methylpent-4-enyl)-pentadec-5-ene (**1**, Scheme 1). This HBI diene has been reported in diatom cultures,<sup>7,18</sup>

and sediments from various regions.<sup>7,8,18-20</sup> It may also result from isomerisation of 2,6,10,14-tetramethyl-7-(3-methylpent-4-enyl)-pentadec-6(17)-ene (IPSO<sub>25</sub>) (**2**) (Scheme 1), a common constituent of Arctic and Antarctic sea ice and surface sediments.<sup>5,12,21,22</sup> Electron ionization (EI) fragmentation pathways of trimethylsilyl (TMS) ethers of (*Z* and *E*) 2,6,10,14-tetramethyl-7-(3-methylpent-4-enyl)-pentadec-5-en-4-ols (**3** and **4**) arising from autoxidation of HBI **1** (Scheme 1) were elucidated by using GC-EI-MS, low-energy collision-induced dissociation (CID)-MS/MS and accurate mass measurements. These compounds were then quantified in Arctic sediment samples in MS/MS multiple reaction monitoring (MRM) mode using transitions based on the main fragmentation pathways elucidated and proposed as valuable tracers of HBI autoxidation in sediments.

## 2. EXPERIMENTAL

### 2.1 Chemicals

A small-scale sample of HBI **1** was obtained from a sediment extract described previously.<sup>8</sup> The sediment extract was further purified here using silver-ion chromatography (Supelco, 250 mg, dichloromethane:acetone (3:1, v/v), 5 mL) to provide a few micrograms of HBI **1** (>93%; GC-MS). HBI **2** (IPSO<sub>25</sub>) (containing approximately 4% of HBI **1**) was obtained from a culture of the marine diatom *Haslea ostrearia* as described previously.<sup>21</sup>

Oxidation of HBI **1** using RuCl<sub>3</sub> and *tert*-butyl hydroperoxide in cyclohexane at room temperature for 16 h<sup>23</sup> and subsequent NaBH<sub>4</sub>-reduction in ether-methanol (4:1, v/v) produced (*Z* and *E*) 2,6,10,14-tetramethyl-7-(3-methylpent-4-enyl)-pentadec-5-en-4-ols (**3** and **4**) in low yield. This method involving oxidation by the bulky *tert*-butyl hydroperoxyl radical avoided oxidation of the sterically hindered allylic C-7.

Treatment of HBI **1** with a stoichiometric amount of perchloroperbenzoic acid in dry dichloromethane (4 h at 50°C) afforded 5,6-epoxy-2,6,10,14-tetramethyl-7-(3-methylpent-4-enyl)-pentadecane (**5**).

The synthesis of the highly structurally related 2,6,10,14,18-pentamethylnonadec-5-en-4-ol (**8**) employed as a standard required two steps: (i) oxidation of (*E*)-phytol (Sigma Aldrich, St. Quentin Fallavier, France) with CrO<sub>3</sub>/pyridine in dry dichloromethane,<sup>24</sup> and (ii) condensation of the resulting (*E*)-phytenal with isobutyl magnesium bromide (Sigma Aldrich, St. Quentin Fallavier, France) in dry diethyl ether. This method strongly favoured 1,2- vs. 1,4-addition.

## 2.2 Autoxidation of HBI **1**

Autoxidation experiments were performed under an atmosphere of air in 15-mL screw-cap flasks containing HBI **1** (amount too low to be weighed) or a mixture of HBIs **1** and **2** (1 mg), *tert*-butyl hydroperoxide (300 ~~μL~~ mL of a 6.0 M solution in decane), di-*tert*-butyl nitroxide (1.2 mg) and hexane (2 mL). After stirring, the flask was incubated in the dark at 65°C. Aliquots (200 μL) were withdrawn from the reaction mixture after incubation for different times. Each sub-sample was evaporated to dryness under a stream of nitrogen and analyzed by gas chromatography–electron ionization mass spectrometry (GC–EI-MS) after NaBH<sub>4</sub> reduction and silylation.

## 2.3 Reduction of oxidation products

Hydroperoxides resulting from HBI oxidation were reduced to the corresponding alcohols by reaction with excess NaBH<sub>4</sub> in diethyl ether:methanol (4:1, v/v) at room temperature (1 h). After reduction, a saturated solution of NH<sub>4</sub>Cl (10 mL) was added cautiously to remove any unreacted reducing agent; the pH was adjusted to 1 with dilute HCl (2 M) and the mixture



135 shaken and extracted with hexane:chloroform (5 mL, 4:1, v/v;  $\times 3$ ). The combined extracts were  
136 dried over anhydrous  $\text{Na}_2\text{SO}_4$ , filtered and evaporated to dryness under a stream of nitrogen.

## 137 2.4 Sampling and treatment of sediments

138 Our sampling location for sediment material corresponds to Barrow Strait (Station 4,  
139  $74^\circ 16' 12''\text{N}$ ,  $91^\circ 46' 12''\text{W}$ , *ca.* 345 m water depth) in the Canadian Arctic. Box cores were  
140 collected, sectioned on board, with sub-samples (1-cm resolution) then freeze-dried before  
141 storage ( $< 4^\circ\text{C}$ ) prior to analysis. The Redox boundary layer was identified previously at *ca.* 2  
142 cm.<sup>16</sup> Sediment sub-samples from sectioned box cores were placed in methanol (15 mL) and  
143 the hydroperoxides were reduced to the corresponding alcohols with excess  $\text{NaBH}_4$  (70 mg, 30  
144 min at  $20^\circ\text{C}$ ). Following the reduction step, water (15 mL) and KOH (1.7 g) were added and  
145 the mixture saponified by refluxing (2 h). After cooling, the contents of the flask were acidified  
146 (HCl, to pH 1) and extracted three times with dichloromethane (30 mL). The combined  
147 dichloromethane extracts were dried over anhydrous  $\text{Na}_2\text{SO}_4$ , filtered and concentrated to give  
148 the total lipid extract (TLE). Since the HBI oxidation product content was quite low relative to  
149 other lipids, accurate quantification required further separation of the TLE using column  
150 chromatography (silica; Kieselgel 60,  $8 \times 0.5$  cm). The HBIs were obtained by elution with  
151 hexane (10 mL) and their oxidation products by subsequent elution with dichloromethane (10  
152 mL).

## 153 2.5 Silylation

154 Dichloromethane eluates of sediments, reduced subsamples of autoxidation experiments  
155 (evaporated to dryness) and standard alcohol **8** were derivatized by dissolving them in 300  $\mu\text{L}$   
156 pyridine/bis-(trimethylsilyl)trifluoroacetamide (BSTFA; Supelco; 2:1, v/v) and silylated ( $50^\circ\text{C}$ ,  
157 1 h). After evaporation to dryness under a stream of  $\text{N}_2$ , the derivatized residue was dissolved  
158 in ethyl acetate/BSTFA (to avoid desilylation) and analysed by mass spectrometric methods.

## 2.6 Gas chromatography/electron ionization tandem mass spectrometry

GC-/EI-MS and GC-/EI-MS/MS experiments were performed using an Agilent 7890A/7000A tandem quadrupole gas chromatograph system (Agilent Technologies, ~~Pare~~ ~~Technopolis~~ ~~—ZA—Courtaboeuf,~~ Les Ulis, France). A cross-linked 5% phenyl-methylpolysiloxane (Agilent; HP-5MS-Ultra Inert) (30 m × 0.25 mm, 0.25 µm film thickness) capillary column was employed. Analyses were performed with an injector operating in pulsed splitless mode set at 270°C and the oven temperature programmed from 70°C to 130°C at 20°C min<sup>-1</sup>, then to 250°C at 5°C min<sup>-1</sup> and ~~then~~ finally to 300°C at 3°C min<sup>-1</sup>. The pressure of the carrier gas (He) was maintained at  $0.69 \times 10^5$  Pa until the end of the temperature program and then programmed from  $0.69 \times 10^5$  Pa to  $1.49 \times 10^5$  Pa at  $0.04 \times 10^5$  Pa min<sup>-1</sup>. The following mass spectrometric conditions were employed: electron energy, 70 eV; transfer line temperature, 300°C; source temperature, 230°C; quadrupole 1 temperature, 150°C; quadrupole 2 temperature, 150°C; collision gas (N<sub>2</sub>) flow rate, 1.5 mL min<sup>-1</sup>; quench gas (He) flow rate, 2.25 mL min<sup>-1</sup>; mass range, m/z 50-700 ~~Dalton~~; cycle time, 313 ms. Collision induced dissociation (CID) was optimized by using collision energies at 5, 10, 15 and 20 eV.

Due to the very low amounts of HBI **1** available, compounds **3** and **4** could not be produced in sufficient amounts to permit quantification, although comparison of their mass fragmentations and retention times with those of compounds detected in sediments allowed their unambiguous identification. Quantification of the TMS ethers of alcohols **3** and **4** was thus carried out with a standard of the highly structurally related 2,6,10,14,18-pentamethylnonadec-5-en-4-ol (**8**; TMS derivative) in multiple reaction monitoring (MRM) mode. A correction factor that took into account the proportion of the selected precursor ion (*m/z* 379 for compounds **3** and **4** and *m/z* 367 for compound **8**) in the EIMS spectra of each compound (Figs-ures 1B and 1C) and that of the selected MRM transition in each CID-MS spectrum was employed.

## 2.7 Gas chromatography/electron ionization quadrupole time of flight mass spectrometry

Accurate mass measurements were carried out in full scan mode with an Agilent 7890B/7200 GC/QTOF System. ~~(Agilent Technologies, Parc Technopolis – ZA Courtaboeuf, Les Ulis, France).~~ A cross-linked 5% phenyl-methylpolysiloxane (Macherey-Nagel, Hoerd, France; Optima-5MS Accent) (30 m × 0.25 mm, 0.25 µm film thickness) capillary column was employed. Analyses were performed with an injector operating in pulsed splitless mode set at 270°C and the oven temperature programmed from 70°C to 130°C at 20°C min<sup>-1</sup> and then to 300°C at 5°C min<sup>-1</sup>. The pressure of the carrier gas (He) was maintained at 0.69 × 10<sup>5</sup> Pa until the end of the temperature program. Instrument temperatures were 300°C ~~for~~for the transfer line and 230°C for the ion source. Nitrogen (flow rate of 1.5 mL min<sup>-1</sup>) was used as the collision gas. Accurate mass spectra were recorded across the range *m/z* 50-700 at 4 GHz with the collision gas valve opened. The QTOF-MS instrument provided a typical resolution ranging from 8009 to 12252 from *m/z* 68.9955 to 501.9706. Perfluorotributylamine (PFTBA) was utilized for daily MS calibration.

198

## 3. RESULTS AND DISCUSSION

### 3.1 Autoxidation of HBI 1

Comparison of retention times and EI mass spectra with those of synthesized standards allowed identification of isomeric (*Z* and *E*) 2,6,10,14-tetramethyl-7-(3-methylpent-4-enyl)-pentadec-5-en-4-ols (**3** and **4**) (Fig. ~~ure~~ure 1B) and 5,6-epoxy-2,6,10,14-tetramethyl-7-(3-methylpent-4-enyl)-pentadecane (**5**) (Fig. ~~ure~~ure 1A) after incubation of HBI **1** in hexane in the presence of *tert*-butyl hydroperoxide (radical enhancer) and di-*tert*-butyl nitroxide (radical initiator)<sup>25</sup> at 65°C and subsequent NaBH<sub>4</sub>-reduction and silylation. Allylic hydrogen abstraction and addition of peroxy radical to the double bonds generally compete during the

208 autoxidation of alkenes.<sup>26</sup> Formation of alcohols **3** and **4** results from hydrogen abstraction at  
209 the allylic C-4 of HBI **1**, and epoxide **5** following peroxy radical addition to the C5-C6 double  
210 bond (Scheme 1). The lack of hydrogen abstraction at the allylic carbon 7 probably results likely  
211 from steric hindrance during hydrogen abstraction by the bulky *tert*-butylperoxy radicals  
212 employed during the incubation.<sup>17</sup>

213 Comparison of autoxidation rates of the two isomeric HBIs **1** and **2** shows that HBI **1** is  
214 oxidized 1.4 times faster than IPSO<sub>25</sub> (**2**). While autoxidation of IPSO<sub>25</sub> (**2**) mainly afforded  
215 1,2-epoxy-2-(4-methylpentyl)-3-(3-methylpent-4-enyl)-6,10-dimethylundecane (**7**) and, to a  
216 lesser extent, 6-methylidene-2,10,14-trimethyl-7-(3-methylpent-4-enyl)-pentadecan-5-ol (**6**)  
217 (ratio **6/7** = 0.1)<sup>17</sup> (Scheme 1), allylic hydrogen abstraction appeared to be more favoured during  
218 autoxidation of HBI **1** (ratio (**3+4**)/**5** = 1.2). This difference in reactivity of allylic C-4 of HBI  
219 **1** and C-5 of IPSO<sub>25</sub> (**2**) towards hydrogen abstraction is in good agreement with EPR  
220 spectroscopy results obtained previously by Camara et al.<sup>27</sup>

221 Due to the well-known lability of epoxides in sediments<sup>17</sup> and during their treatment,<sup>28</sup>  
222 the production of a higher proportion of allylic alcohols **3** and **4** during autoxidation of HBI **1**  
223 strengthens the tracer potential of autoxidation products of this alkene.

### 225 3.2 EIMS fragmentations of 2,6,10,14-tetramethyl-7-(3-methylpent-4-enyl)-pentadec- 226 5(*Z/E*)-en-4-ol TMS ether derivatives (**3** and **4**)

227 The TMS ethers of the *Z* and *E* isomers **3** and **4** exhibited the same EI mass spectra (Fig-  
228 ure 1B), with weak peaks at *m/z* 436 and *m/z* 421 corresponding to the molecular ion (**a**<sup>+</sup>) and  
229 [M – CH<sub>3</sub>]<sup>+</sup> (**b**<sup>+</sup>), respectively. Intense and interesting peaks were also observed at *m/z* 379, ~~*m/z*~~  
230 289, ~~*m/z*~~ 199, ~~*m/z*~~ 163, ~~*m/z*~~ 143 and ~~*m/z*~~ 109. α-Cleavage relative to the ionized ether group  
231 affords fragment ion **c**<sup>+</sup> at *m/z* 379, which may lose a neutral molecule of trimethylsilanol  
232 (TMSOH) after 1,5-hydrogen shift from C-17 to the ionized ether group. Subsequent 1,4-

cyclization yields ion **d**<sup>+</sup> at  $m/z$  289 (Scheme 2), which can then be cleaved to the fragment ion **e**<sup>+</sup> at  $m/z$  163 following 1,5-hydrogen shift from C-10 to the charged cyclobutyl ring and concerted ring extension (Scheme 2). Cleavage of ion **f**<sup>+</sup> at  $m/z$  379 (mesomer of ion **c**<sup>+</sup>) involving a 1,3-hydrogen shift from C-8 to the carbocation may be at the origin of the formation of the strongly stabilized ion **g**<sup>+</sup> at  $m/z$  143 (Scheme 2).

Ionization of TMS ethers of the *Z* and *E* isomers **3** and **4** can also take place at the 5-6 double bond affording ion **h**<sup>+</sup> at  $m/z$  436, which can be cleaved to the strongly stabilized ion **i**<sup>+</sup> at  $m/z$  199 after a 1,3-hydrogen shift from C-4 to the ionized tertiary C-6 and subsequent cleavage of the C6-C7 bond (Scheme 2). Ion **i**<sup>+</sup> can then either lose a neutral molecule of TMSOH after a 1,3-hydrogen shift from C-17 and subsequent 1,4-cyclization to produce the fragment ion **j**<sup>+</sup> at  $m/z$  109, or be converted to ion **g**<sup>+</sup> at  $m/z$  143 following a 1,3-hydrogen shift from tertiary C-2 and cleavage of the C3-C4 bond (Scheme 2).

The proposed fragmentation pathways are supported further by the results of CID analyses of precursor ions **a**<sup>+</sup> and **h**<sup>+</sup> at  $m/z$  436, **c**<sup>+</sup> and **f**<sup>+</sup> at  $m/z$  379, **d**<sup>+</sup> at  $m/z$  289 and **i**<sup>+</sup> at  $m/z$  199 (Table 1). Moreover, the accurate masses of ions **a**<sup>+</sup>-**j**<sup>+</sup> showed only minor deviations (ranging from 0.7 to 5.7 ppm) from the calculated theoretical masses (Table 2), thus confirming the elemental composition of the fragment ions in each case.

### 3.3 MRM quantification of compounds **3** and **4** in sediment samples

The mass spectral transitions employed for the quantification of oxidation products were  $m/z$  379 → 143 for TMS ethers of compounds **3** and **4**, and  $m/z$  367 → 143 for the TMS ether of the standard **8**. Transitions  $m/z$  379 → 163 and  $m/z$  379 → 289 were used as qualifiers (i.e. to confirm qualitatively the presence of TMS ethers of compounds **3** and **4**). It may be noted that transitions resulting from the cleavage of ion **i**<sup>+</sup> at  $m/z$  199 appeared to be insufficiently specific for the analysis of sediment extracts and were thus discarded.

The limit of quantification (150 pg) was determined according to a signal-to-noise ratio greater than 3. The linear range was determined using values that met the standard analysis criteria of less than 15% deviation across the concentration range. Linear responses were obtained over 2 to 3 orders of magnitude. Due to: (i) the relatively low amounts of sediments available and (ii) the low concentrations of analytes, the reproducibility of our analyses could not be determined. Despite the relatively weak concentration of HBI **1** in sediments from Barrow Strait (Table 3), compounds **3** and **4** could be readily detected and quantified (Table 3, Figure 2). It is interesting to note that the detection of these compounds, which eluted just after phytol (chlorophyll phytyl side chain) TMS ether, is also possible by GC-QTOF (by extracting the accurate mass of ion  $f^+$ ) but not by GC-EI-MS (due to the complexity of the organic extracts of sediments). The proportion of such allylic alcohols relative to the parent HBI (up to 26%) (Table 3) appeared to be two orders of magnitude higher than that of the alcohol **6** relative to the parent IPSO<sub>25</sub> (**2**) in the same sediments (up to 0.2%)<sup>17</sup>. The decrease of the ratio **3/4** observed in sediments relative to the autoxidation experiment (Figure 2) was attributed to allylic rearrangement of the corresponding hydroperoxides to 2,6,10,14-tetramethyl-7-(3-methylpent-4-enyl)-pentadec-4(*E*)-en-6-hydroperoxide (**9**) (Scheme 1) inhibited by high concentration of *tert*-butyl-hydroperoxide during the autoxidation experiment<sup>25</sup> but not in sediments. Indeed, it was previously observed that rearrangement of *E*-allylperoxyls was reversible, but this was not the case for *Z*-allylperoxyls<sup>29</sup> (Scheme 1).

#### 4. CONCLUSIONS

The main autoxidation products of the HBI diene 2,6,10,14-tetramethyl-7-(3-methylpent-4-enyl)-pentadec-5-ene (**1**) were identified as (*Z* and *E*) 2,6,10,14-tetramethyl-7-(3-methylpent-4-enyl)-pentadec-5-en-4-ols (**3** and **4**) and 5,6-epoxy-2,6,10,14-tetramethyl-7-(3-methylpent-4-enyl)-pentadecane (**5**). CID-MS/MS and accurate mass measurements allowed

the EI mass fragmentations of TMS ethers of alcohols **3** and **4** to be elucidated. On the basis of these fragmentations, some MRM transitions were selected and applied to lipid extracts of Arctic sediments. Although the reproducibility of analyses could not be determined, these compounds appeared to be present in quite high proportions relative to the parent HBI (**1**) (up to 26%). The apparent stability of compounds **3** and **4** in sediments, their production in high proportion during autoxidation of HBI **1** and the potential isomerization of the widely distributed IPSO<sub>25</sub> (**2**) to their parent HBI **1** under environmental conditions supports the use of these alcohols as tracers of HBI autoxidation in sediments.

291

## 292 ACKNOWLEDGEMENTS

293 Financial support from the Centre National de la Recherche Scientifique (CNRS) and the  
294 Aix-Marseille University is gratefully acknowledged. Thanks are due to the FEDER  
295 OCEANOMED (N° 1166-39417) for the funding of the apparatus employed. We are grateful  
296 to L. Vare, G. Massé, A. Rochon and the officers and crew of the CCGS Amundsen for help  
297 with obtaining box core sediment material. We thank three anonymous reviewers for their  
298 helpful and constructive comments.

299

## 300 REFERENCES

301

- 302 [1] Volkman JK, Barrett SM, Dunstan GA. C<sub>25</sub> and C<sub>30</sub> highly branched isoprenoid alkenes in  
303 laboratory cultures of two marine diatoms. *Org Geochem.* 1994; 21: 407-414.  
304 [2] Sinninghe Damsté JS, Schouten S, Rijpstra WIC, et al. Structural identification of the C<sub>25</sub>  
305 highly branched isoprenoid pentaene in the marine diatom *Rhizosolenia setigera*. *Org*  
306 *Geochem.* 1999; 30: 1581-1583.



- [3] Belt ST, Massé G, Allard WG, Robert J-M, Rowland SJ. Identification of a C<sub>25</sub> highly branched isoprenoid triene in the freshwater diatom *Navicula sclesvicensis*. *Org Geochem*. 2001a; 32: 1169-1172.
- [4] Belt ST, Massé G, Allard WG, Robert J-M, Rowland SJ. C<sub>25</sub> highly branched isoprenoid alkenes in planktonic diatoms of the *Pleurosigma* genus. *Org Geochem* 2001b; 32: 1271-1275.
- [5] Belt ST, Smik L, Brown TA, et al. Source identification and distribution reveals the potential of the geochemical Antarctic sea ice proxy IPSO<sub>25</sub>. *Nature Commun* 2016; 7: 12655.
- [6] Grossi V, Beker B, Geenevasen JAJ, et al. C<sub>25</sub> highly branched isoprenoid alkenes from the marine benthic diatom *Pleurosigma strigosum*. *Phytochem*. 2004; 65: 3049-3055.
- [7] Brown TA, Belt ST, Tatarek A, Mundy CJ. Source identification of the Arctic sea ice proxy IP<sub>25</sub>. *Nature Commun*. 2014; 5: 4197.
- [8] Kaiser J, Belt ST, Tomczak T, Brown TA, Wasmund N, Arz HW. C<sub>25</sub> highly branched isoprenoid alkenes in the Baltic Sea produced by the marine planktonic diatom *Pseudosolenia calcar-avis*. *Org Geochem*. 2016; 93: 51-58.
- [9] Rowland SJ, Hird SJ, Robson JN, Venkatesan MI. Hydrogenation behaviour of two highly branched C<sub>25</sub> dienes from Antarctic marine sediments. *Org Geochem*. 1990; 15: 215-218.
- [10] Belt ST, Allard WG, Massé G, Robert J-M, Rowland SJ. Highly branched isoprenoids (HBIs): identification of the most common and abundant sedimentary isomers. *Geochim Cosmochim Acta*. 2000; 64: 3839-3851.
- [11] Sinninghe Damsté JS, Muyzer G, Abbas B, et al. The rise of the rhizosolenid diatoms. *Science*. 2004; 304: 584-587.
- [12] Belt ST. Source-specific biomarkers as proxies for Arctic and Antarctic sea ice. *Org Geochem*. 2018; 125: 277-298.



- [13] Rontani J-F, Belt ST, Vaultier F, Brown TA. Visible light-induced photooxidation of highly branched isoprenoid (HBI) alkenes: a significant dependence on the number and nature of the double bonds. *Org Geochem.* 2011; 42: 812-~~822~~.
- [14] Rontani J-F, Belt ST. Photo- and autoxidation of unsaturated algal lipids in the marine environment: an overview of processes, their potential tracers, and limitations. *Org Geochem* 20~~20~~19; 139: 10394~~1~~.~~1~~.
- [15] Rontani J-F, Belt S, Vaultier F, Brown T, Massé G. Autoxidative and photooxidative reactivity of highly branched isoprenoid (HBI) alkenes. *Lipids.* 2014; 49: 481-~~494~~.
- [16] Rontani J-F, Belt ST, Amiraux R. Biotic and abiotic degradation of the sea ice diatom biomarker IP<sub>25</sub> and selected algal sterols in near-surface Arctic sediments. *Org Geochem* 2018; 118: 73-~~88~~.
- [17] Rontani J-F, Smick L, Belt ST. Autoxidation of the sea ice biomarker proxy IPSO<sub>25</sub> in the near-surface oxic layers of Arctic and Antarctic sediments. *Org Geochem.* 2019; 129: 63-~~76~~.
- [18] Massé G, Belt ST, Rowland SJ, Rohmer M. Isoprenoid biosynthesis in the diatoms *Rhizosolenia setigera* (Brightwell) and *Haslea ostrearia* (Simonsen). *Proc Nat Acad Sci.* ~~USA~~2004; ~~101~~: 4413-~~4418~~.
- [19] Belt ST, Cooke DA, Hird SJ, Rowland SJ. Structural Determination of a Highly Branched C<sub>25</sub> Sedimentary Isoprenoid Biomarker by NMR Spectroscopy and Mass Spectrometry. *J Chem Soc Chem Commun.* 1994; 2077-~~2078~~.
- [20] Xu Y, Jaffé R, Wachnicka A, Gaiser EE. Occurrence of C<sub>25</sub> highly branched isoprenoids (HBIs) in Florida Bay: paleoenvironmental indicators of diatom-derived organic matter inputs. *Org Geochem.* 2006; 37: 847-~~859~~.

- [21] Johns L, Wraige EJ, Belt ST<sub>2</sub> et al. Identification of a C<sub>25</sub> highly branched isoprenoid (HBI) diene in Antarctic sediments, Antarctic sea-ice diatoms and cultured diatoms. *Org Geochem.* 1999; 30: 1471-1475.
- [22] Amiraux R, Smik L, Köseoglu D<sub>2</sub> et al. Temporal evolution of IP<sub>25</sub> and other highly branched isoprenoid lipids in sea ice and the underlying water column during an Arctic melting season. *Elem Sci Anth.* 2019; 7(1):38. doi.org/10/1525/elementa.377.
- [23] Seki H, Ohyama K, Sawai S<sub>2</sub> et al. Licorice β-amyrin 11-oxidase, a cytochrome P450 with a key role in the biosynthesis of the triterpene sweetener glycyrrhizin. *Proc Natl Acad Sci USA* 2008; 105: 14204-14209.
- [24] Gellerman JL, Anderson WH, Schlenck H. Synthesis and analysis of phytol and phytinoyl wax esters. *Lipids.* 1975; 10: 656-661.
- [25] Porter NA, Caldwell SE, Mills KA. Mechanisms of free radical oxidation of unsaturated lipids. *Lipids.* 1995; 30: 277-290.
- [26] Schaich KM. Lipid oxidation: theoretical aspects. In: Shahidi, F. (Ed.), *Bailey's industrial oil and fat products*. John Wiley & Sons, Chichester, 2005.
- [27] Camara S, Gilbert BC, Meier RJ, van Duin M, Whitwood AC. EPR and modelling studies of hydrogen-abstraction reactions relevant to polyolefin cross-linking and grafting chemistry. *Org Biomol Chem.* 2003; 1:1181-1190.
- [28] Marchand D, Rontani J-F. Characterisation of photooxidation and autoxidation products of phytoplanktonic monounsaturated fatty acids in marine particulate matter and recent sediments. *Org Geochem.* 2001; 32: 287-304.
- [29] Porter NA, Mills KA, Carter RL. A mechanistic study of oleate autoxidation: Competing peroxy H-atom abstraction and rearrangement. *J Am Chem Soc.* 1994; 116: 6690-6696.

FIGURE AND SCHEME CAPTIONS

**Figure 1.** EI mass spectra of 5,6-epoxy-2,6,10,14-tetramethyl-7-(3-methylpent-4-enyl)-pentadecane (**5**) (A), 2,6,10,14-tetramethyl-7-(3-methylpent-4-enyl)-pentadec-5(*E*)-en-4-ol TMS derivative (**4**) (B) and 2,6,10,14,18-pentamethylnonadec-5-en-4-ol TMS derivative (**8**) (C).

**Figure 2.** MRM chromatograms ( $m/z$  379  $\rightarrow$  143,  $m/z$  379  $\rightarrow$  163 and  $m/z$  379  $\rightarrow$  289) of silylated HBI **1** autoxidation products **3** and **4** (produced during autoxidation experiment) (A) and DCM fraction obtained from the 2-3 cm (B) and 10-11 cm (C) layer of the core sediment from Barrow Strait.

**Scheme 1.** Autoxidation and interconverting of HBI dienes **1** and **2**.

**Scheme 2.** Proposed fragmentation mechanisms of alcohols **3** and **4** TMS derivatives.

**Table 1.** CID analyses of the different fragment ions.

Code	<i>m/z</i>	Collision energy (eV)	Product ions
<b>i<sup>+</sup></b>	199	5	199(100), 181(8), 157(5), 143(41), 129(7), 109(19), 99(9), 87(6), 75(38), 73(36)
<b>d<sup>+</sup></b>	289	5	289(100), 199(23), 171(24), 163(45), 149(33), 127(14), 121(26), 107(29), 97(13), 95(26), 83(19), 81(39)
<b>c<sup>+</sup> and f<sup>+</sup></b>	379	5	379(100), 289(17), 269(11), 163(49), 149(14), 143(40), 129(17), 121(11), 109(22), 107(18), 103(14), 95(25), 81(18), 69(15)
<b>a<sup>+</sup> and h<sup>+</sup></b>	436	7	436(100), 379(37), 295(4), 275(6), 253(45), 225(30), 199(75), 129(23), 69(5)

**Table 2.** High-accuracy mass spectral data for ions **a<sup>+</sup>-j<sup>+</sup>**

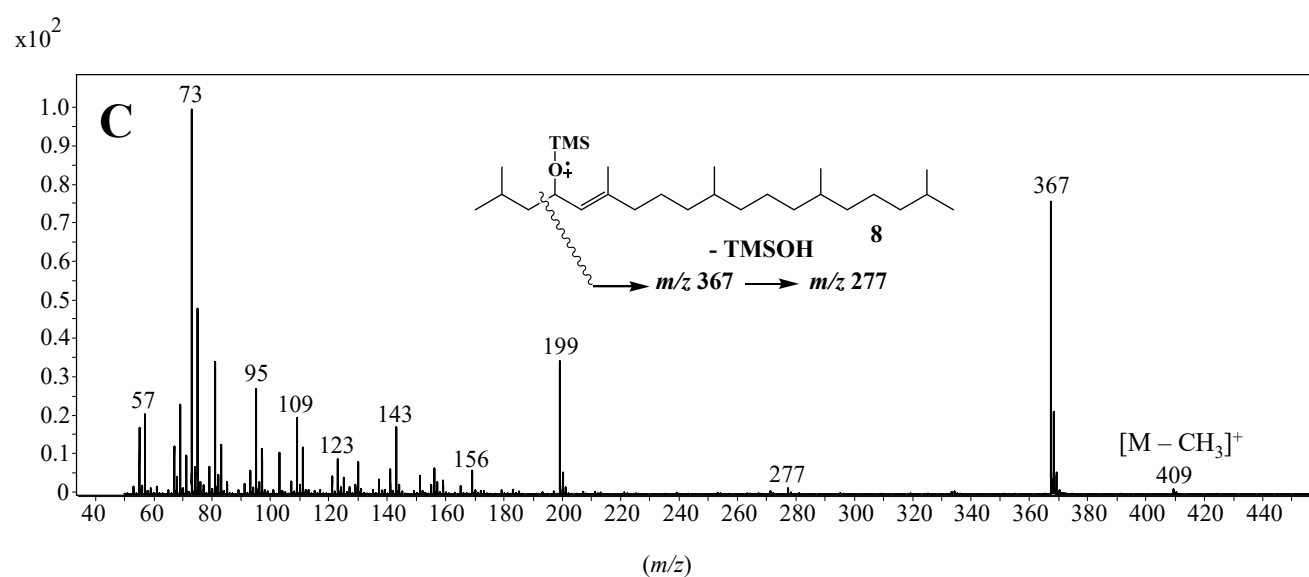
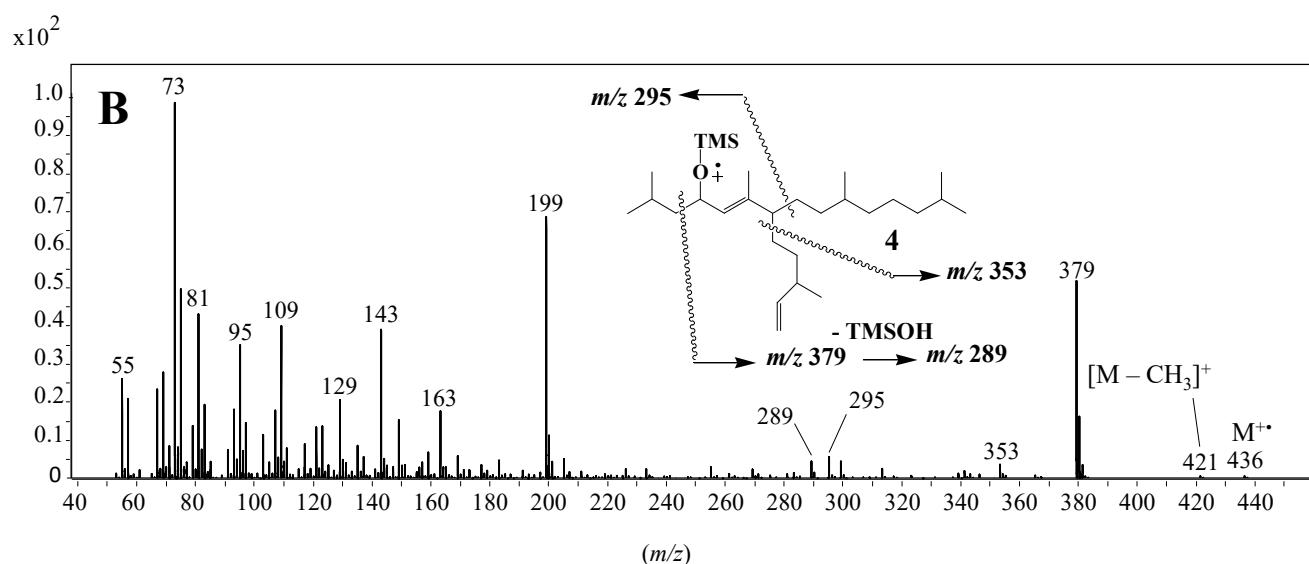
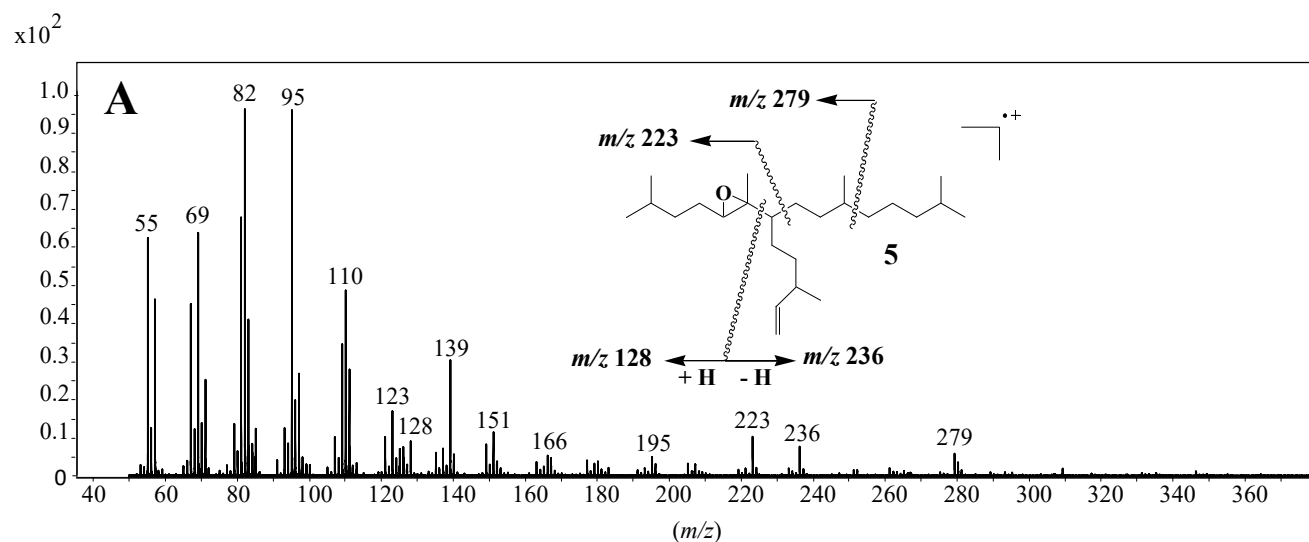
Code	Formula	<i>m/z</i> calculated	<i>m/z</i> observed	Δ (ppm)
j <sup>+</sup>	C <sub>8</sub> H <sub>13</sub>	109.1012	109.1011	-0.9
g <sup>+</sup>	C <sub>7</sub> H <sub>15</sub> OSi	143.0887	143.0886	-0.7
e <sup>+</sup>	C <sub>12</sub> H <sub>19</sub>	163.1481	163.1485	+2.4
i <sup>+</sup>	C <sub>11</sub> H <sub>23</sub> OSi	199.1513	199.1516	+1.5
d <sup>+</sup>	C <sub>21</sub> H <sub>37</sub>	289.2890	289.2896	+2.1
c <sup>+</sup> and f <sup>+</sup>	C <sub>24</sub> H <sub>47</sub> OSi	379.3391	379.3401	+2.6
b <sup>+</sup>	C <sub>27</sub> H <sub>53</sub> OSi	421.3890	421.3866	-5.7
a <sup>+</sup> and h <sup>+</sup>	C <sub>28</sub> H <sub>56</sub> OSi	436.4095	436.4102	+1.6

**Table 3.** Concentration of HBI **1** and its autoxidation products **3** and **4** in sediments from the Arctic station 4 (Barrow Strait)

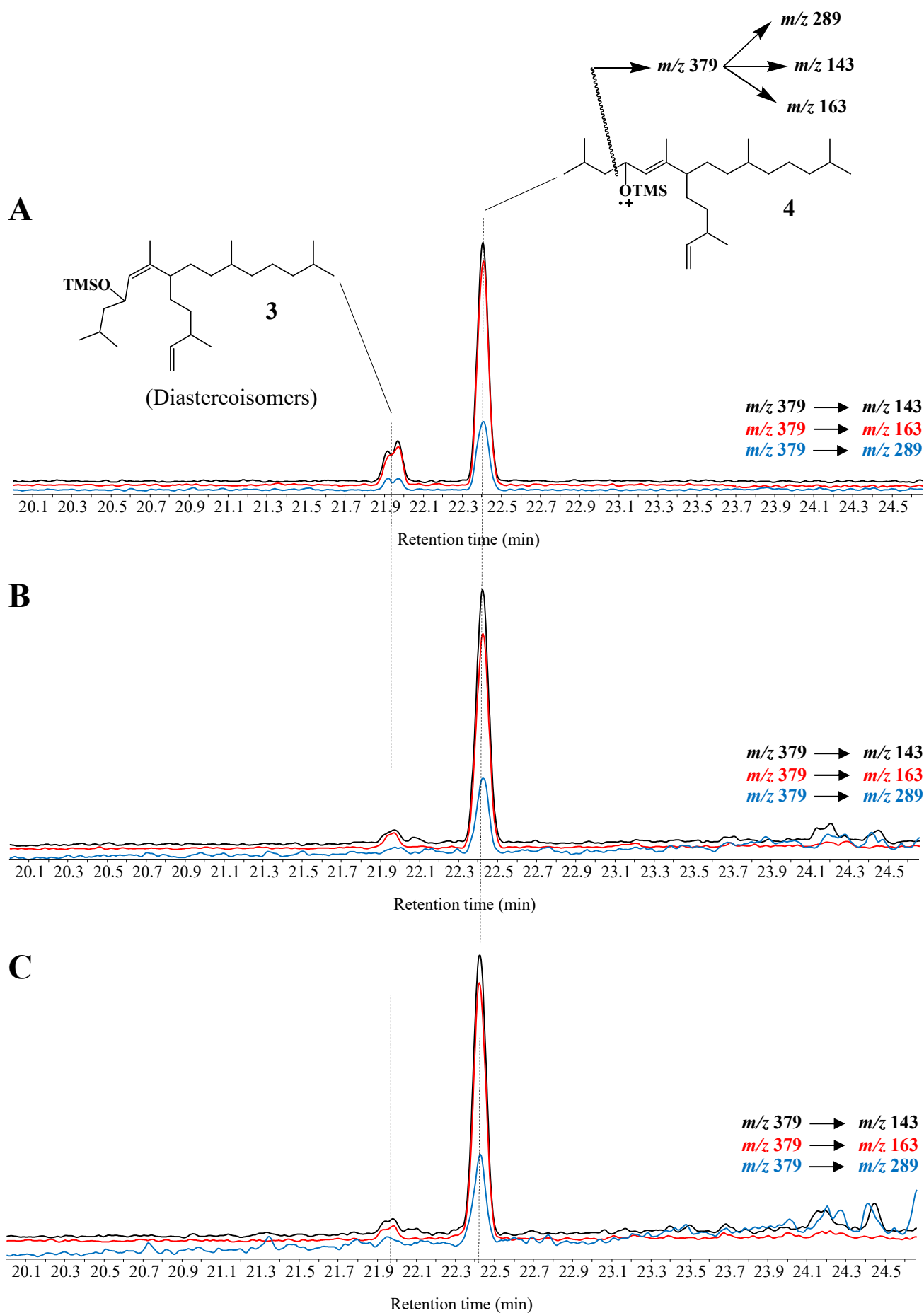
Depth (cm)	HBI <b>1</b> ( $\mu\text{g g}^{-1}$ )	Compound <b>3</b> ( $\text{ng g}^{-1}$ )	Compound <b>4</b> ( $\text{ng g}^{-1}$ )	Total ( <b>3</b> + <b>4</b> ) ( $\text{ng g}^{-1}$ )	( <b>3</b> + <b>4</b> )/ <b>1</b> (%)
1-2	0.19	4.0	15.6	19.6	10
2-3	0.32	2.0	19.6	21.6	7
4-5	0.31	4.6	43.4	48.0	16
6-7	0.27	3.8	42.6	46.4	17
8-9	0.16	Tr*	9.6	9.6	6
10-11	0.22	16.2	41.2	57.4	26

\* Traces (< LOD)

"Disclaimer: This is a pre-publication version. Readers are recommended to consult the full published version for accuracy and citation."

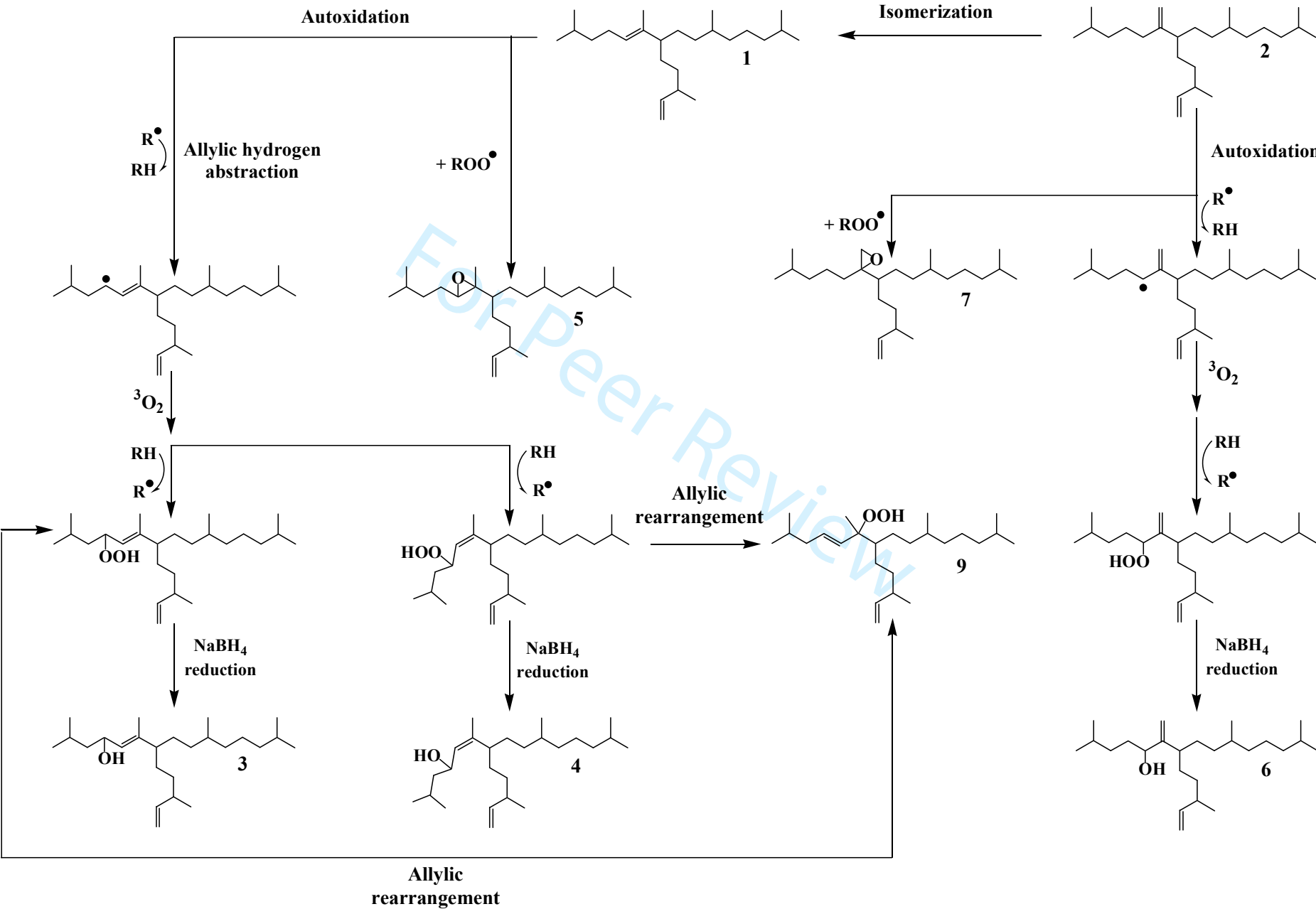


"Disclaimer: This is a pre-publication version. Readers are recommended to consult the full published version for accuracy and citation."





“ Disclaimer: This is a pre-publication version. Readers are recommended to consult the full published version for accuracy and citation.”



"Disclaimer: This is a pre-publication version. Readers are recommended to consult the full published version for accuracy and citation."

